MODEL-BASED ADAPTIVE DETECTION OF RANGE-SPREAD TARGETS

G. Alfano A. De Maio A. Farina

May 2003

G. Alfano and A. De Maio are with the Dipartimento di Ingegneria Elettronica e delle Telecomunicazioni, Università degli Studi di Napoli "Federico II", Via Claudio 21, I-80125 Napoli, Italy. E-mail: a.demaio@unina.it

A. Farina is with Alenia Marconi Systems, via Tiburtina Km.12.4, 00131, Roma, Italy. E-mail: afarina@amsjv.it

Abstract

In this paper we consider the problem of detecting range-distributed targets in the presence of structured disturbance modeled as an autoregressive Gaussian process with unknown parameters. We focus on two different scenarios. The former assumes that all the data vectors from the cells under test share the same covariance matrix (homogeneous environment). The latter refers to the case of data vectors characterized by completely different covariances (heterogeneous environment). We devise and assess four detectors exploiting the asymptotic generalized likelihood ratio criterion. Remarkably they ensure the Constant False Alarm Rate (CFAR) property with respect to the disturbance power level and two of them are asymptotically CFAR with respect to the disturbance covariance matrix. Finally the performance assessment, based also on real radar data, has shown that the newly devised detectors achieve in general satisfactory detection performances.

1 Introduction

In the past few years the problem of detecting range-distributed targets has received more and more attention [1]. It naturally arises when considering detection with High Resolution Radars [2, 3] capable of resolving a target into a number of scattering centers appearing into different range cells [4]. Moreover, it is also well known that the point-target model may fail in many practical scenarios wherein a low/medium resolution radar is employed: examples of these situations are the detection of large ships with coastal radars, and that of a cluster of point-targets flying at the same velocity in close spatial proximity to one another. The adaptive detection of range-distributed targets has already been handled in [5, 6, and references therein] with reference to targets embedded in Gaussian disturbance with unknown covariance matrix. Therein it is assumed that data are collected by N sensors and the possible target is contained within H range cells. Moreover, in [6], it is also supposed the existence of K secondary data vectors free of target components. Both the approaches employ the assumption that interference returns are independent and identically distributed Gaussian vectors (homogeneous environment), and lead to detectors achieving satisfactory performance when $H > 2N$ (for [5]) and $K > 2N$ (for [6]).

Unfortunately experimental campaigns have demonstrated that for reasonable values of N the assumption of $H > 2N$ or $K > 2N$ homogeneous data is not always verified [7]. Additionally, the analysis of several Space-Time Adaptive Processing (STAP) algorithms, mostly conducted assuming homogeneity of the secondary data, has shown that inhomogeneities magnify the loss between the adaptive implementation and optimum conditions [8, 9, 10]. It is thus possible that the homogeneous model does not adequately describe the actual radar scenario; in these situations it can be thought of resorting to data selection techniques in order to collect secondary samples. To this end techniques, relying on knowledge-based criteria, have been proposed in [11]. In [12], instead, two data-adaptive methodologies, called "Power Selected Training" and "Power Selected Deemphasis", for selecting the training data set are proposed and assessed on recorded radar data. A quite different strategy to cope with the lack of a huge amount of homogeneous data could be that of exploiting the structural information about the disturbance covariance. By doing so, we get a reduction in the number of parameters to be estimated so that the amount of data required for achieving good estimation performance could be significantly reduced thus decreasing the uncertainty in learning. This approach has been followed in [13] where the covariance of the interference has been modeled as the sum of an unknown positive semidefinite matrix plus a known full rank one.

In this paper we still consider the case of structured interference. More precisely the proposed approach relies on modeling the overall disturbance as an autoregressive (AR) Gaussian process. The reasons for using this model are reported in the sequel [14]:

- For a wide-sense stationary process with Power Spectral Density (PSD) $S(f)$ and for any $\epsilon > 0$ there exist an AR PSD $S_{AR}(f)$ such that at every frequency the error made replacing $S(f)$ by $S_{AR}(f)$ is at most ϵ.

- Given N values of the disturbance covariance, the PSD that corresponds to the most random or the most unpredictable time series whose covariance function agrees with the known values is the AR PSD whose coefficients are computed solving a set of linear equations known as the Yule-Walker equations (Maximum Entropy Method (MEM)).

- It is well known that in many situations of practical interest, the interference can be modeled as an AR process of relatively low order M. Specifically, in radar echo modeling, M ranges from 2 to 5, whereas in active sonar environment M is usually chosen equal to 8 [14, pp. 16].

Previous works in the field of radar signal processing involving AR processes concern mainly the problem of designing adaptive clutter cancellators. In particular in [15, 16] the MEM approach is invoked for devising adaptive clutter filters exploiting the Burg algorithm. In [17], instead, the authors resort to the Kalman filtering technique for estimating the AR coefficients and thus develop adaptive filter structures achieving a fast adaptivity even for the cases in which the clutter Doppler frequency changes significantly over short range intervals.

With reference to the problem of detecting point-like targets, the AR model is exploited in [18], for the case of known target echo, in [14] for the detection of an AR process in the presence of disturbance still modeled as an AR process with different coefficients, and in [19] for the detection of a target signal known up to a scaling factor. Finally, more recently, the use of multichannel AR processes for radar STAP applications has been proposed in [20, 21] for point-like targets embedded in a Gaussian environment, and in [22] for the case of non-Gaussian disturbance.

In this paper, for the first time, we attack the problem of detecting range spread targets in the presence of disturbance modeled as an AR process with unknown parameters. More specifically we focus on two radar scenarios of relevant practical interest: the former assumes that all the data vectors share the same covariance matrix, whereas the latter considers the case of a totally inhomogeneous environment where the data from the cells under test possess completely different covariances. In both situations we do not suppose the presence of training data and devise detection structures which are asymptotic expressions of the Generalized Likelihood Ratio Test (GLRT). Remarkably all the proposed receivers ensure the CFAR property with respect to the disturbance power level and two of them are also asymptotically CFAR with respect to the disturbance covariance.

The paper is organized as follows. Section 2 is focused on the problem formulation and the design of the novel detectors. Section 3 contains the performance assessment, conducted also with the aid of real data collected by the IPIX radar. Finally, conclusions are drawn in Section 4.

2 Problem Formulation and System Design

We assume that data are the returns from a coherent pulse train composed of N pulses and deal with the problem of detecting the presence of a target across H range cells. We denote by z_t, $t = 1, \ldots, H$, the N-dimensional vector of the returns from the t-th range cell and neglect range migration[1].

The detection problem to be solved can be formulated in terms of the following binary

[1] Notice that if the range resolution Δ_r is greater than 3 m and the CPI is smaller than 1 msec than the range migration can be neglected if the target velocity is smaller than 500 m/sec. [23].

hypotheses test:

$$\begin{cases} H_0: \ z_t = \mathbf{n}_t, \qquad t = 1, \ldots, H \\ H_1: \ z_t = \alpha_t \ \boldsymbol{p} + \mathbf{n}_t, \qquad t = 1, \ldots, H \end{cases} \tag{1}$$

where $\boldsymbol{p} = [1, e^{j2\pi f_d}, \ldots, e^{j2\pi(N-1)f_d}]^T$ denotes the N-dimensional steering vector, $(\cdot)^T$ denotes transpose, f_d is the normalized target Doppler, and the α_t's, $t = 1, \ldots, H$, are (unknown) deterministic parameters accounting for both the target and the channel propagation effects. As to the disturbance vectors, we assume that the $\mathbf{n}_t$'s, $t = 1, \ldots, H$, are N-dimensional complex vectors, samples from independent, AR Gaussian processes of order M. Precisely the k-th component of $\mathbf{n}_t$, $\mathbf{n}_t(k)$, is given by

$$\mathbf{n}_t(k) = \sum_{l=1}^{M} \mathbf{a}_t(l)\mathbf{n}_t(k-l) + w_t(k) \qquad k = 1, \ldots, N \tag{2}$$

where $\mathbf{a}_t = [\mathbf{a}_t(1), \ldots, \mathbf{a}_t(M)]$ is the complex M-dimensional vector of the AR parameters and $w_t(k)$ is a sequence of independent and identically distributed complex Gaussian random variables with zero-mean and variance σ_t^2 [2].

In the sequel we consider two different scenarios. The former, referred to as homogeneous environment, assumes that the interference vectors share the same covariance, i.e. $\mathbf{a}_t = \mathbf{a}$ and $\sigma_t^2 = \sigma^2$, $t = 1, \ldots, H$. The latter, instead, deals with the case where the vectors $\mathbf{n}_t$, $t = 1, \ldots, H$, have a completely different covariance matrix (heterogeneous environment). According to the Neyman-Pearson criterion, the optimum solution to the hypotheses testing problem (1), is the likelihood ratio test; but, for the cases under consideration, it cannot be employed since total ignorance of the parameters $\mathbf{a}, \sigma^2, \alpha_1, \ldots, \alpha_H$ for the homogeneous environment, and $\mathbf{a}_1, \ldots, \mathbf{a}_H, \sigma_1^2, \ldots, \sigma_H^2, \alpha_1, \ldots, \alpha_H$ for the heterogeneous scenario is assumed. A possible way to cope with the aforementioned *a priori* uncertainty relies on exploiting the Generalized Likelihood Ratio Test (GLRT), which is tantamount to replacing the unknown parameters by their maximum likelihood estimates under each hypothesis [1]. Unfortunately, the decision statistic based on the above algorithm does not admit a closed form expression. In fact the exact maximization with respect to the

[2]Notice that the derivations which follow apply also to the case of disturbance vectors n_t modeled as samples of an autoregressive Spherically Invariant Random Process (SIRP) [24, 25].

This is tantamount to assuming that the driving process $w_t(k)$ can be written as the product of a nonnegative random variable, referred to in the sequel as *texture*, times a Gaussian white process $g_t(k)$.

AR parameters produces a set of highly nonlinear equations [26]. However, for large data records, the probability density function (pdf) of the data vectors can be suitably approximated and, thus, it is possible to come up with a closed form expression for the maximum likelihood estimates. Precisely, denoting with $f(\,\boldsymbol{z}_t|\mathbf{a}_t, \sigma_t^2, H_0)$ and $f(\,\boldsymbol{z}_t|\mathbf{a}_t, \sigma_t^2, \alpha_t, H_1)$ the pdf's of the vectors[3] $\boldsymbol{z}_t$, $t = 1, \dots, H$, under H_0 and H_1, it can be shown [14] that for $N \gg M$

$$f(\,\boldsymbol{z}_t|\mathbf{a}_t, \sigma_t^2, H_0) = \frac{1}{(\pi\sigma_t^2)^{(N-M)}} \exp\left\{-\frac{1}{\sigma_t^2}(\,\boldsymbol{u}_t - \,\boldsymbol{Z}_t\mathbf{a}_t)^\dagger(\,\boldsymbol{u}_t - \,\boldsymbol{Z}_t\mathbf{a}_t)\right\} \tag{3}$$

$$f(\,\boldsymbol{z}_t|\mathbf{a}_t, \sigma_t^2, \alpha_t, H_1) =$$

$$\frac{1}{(\pi\sigma_t^2)^{(N-M)}} \exp\left\{-\frac{1}{\sigma_t^2}(\,\boldsymbol{u}_t - \alpha_t\,\boldsymbol{q} - \,\boldsymbol{Z}_t\mathbf{a}_t - \alpha_t\,\boldsymbol{P}\mathbf{a}_t)^\dagger(\,\boldsymbol{u}_t - \alpha_t\,\boldsymbol{q} - \,\boldsymbol{Z}_t\mathbf{a}_t - \alpha_t\,\boldsymbol{P}\mathbf{a}_t)\right\} \tag{4}$$

where $(\cdot)^\dagger$ denotes conjugate transpose, $\boldsymbol{u}_t = [\,\boldsymbol{z}_t(M+1), \dots,\,\boldsymbol{z}_t(N)]^T$, $\boldsymbol{q} = [\,\boldsymbol{p}(M+1), \dots,\,\boldsymbol{p}(N)]^T$,

$$\boldsymbol{Z}_t = \begin{pmatrix} \boldsymbol{z}_t(M) & \boldsymbol{z}_t(M-1) & \dots & \boldsymbol{z}_t(1) \\ \boldsymbol{z}_t(M+1) & \boldsymbol{z}_t(M) & \dots & \boldsymbol{z}_t(2) \\ \vdots & \vdots & \ddots & \vdots \\ \boldsymbol{z}_t(N-1) & \boldsymbol{z}_t(N-2) & \dots & \boldsymbol{z}_t(N-M) \end{pmatrix}$$

$$\boldsymbol{P} = \begin{pmatrix} \boldsymbol{p}(M) & \boldsymbol{p}(M-1) & \dots & \boldsymbol{p}(1) \\ \boldsymbol{p}(M+1) & \boldsymbol{p}(M) & \dots & \boldsymbol{p}(2) \\ \vdots & \vdots & \ddots & \vdots \\ \boldsymbol{p}(N-1) & \boldsymbol{p}(N-2) & \dots & \boldsymbol{p}(N-M) \end{pmatrix}$$

Remarkably we will prove that the maximization of (3) and (4) with respect to the unknown parameters leads to closed form expression for the estimates. Hence this last consideration justifies the use of the above pdf's for evaluating the Asymptotic GLRT (AGLRT).

[3]Note that equations (3) and (4) refer to the heterogeneous scenario. However letting $\mathbf{a}_t = \mathbf{a}$ and $\sigma_t^2 = \sigma^2$, $t = 1, \dots, H$ we come up with the pdf's for the homogeneous case.

2.1 Homogeneous Environment

Assuming that $\mathbf{a}$ and σ^2 are unknown parameters we solve the hypotheses test (1) resorting to the AGLRT, namely we consider the following decision rule

$$\frac{\max_{\sigma^2, \boldsymbol{\alpha}, \mathbf{a}} f(\boldsymbol{z}_1, \ldots, \boldsymbol{z}_H | \mathbf{a}, \sigma^2, \boldsymbol{\alpha}, H_1)}{\max_{\sigma^2, \mathbf{a}} f(\boldsymbol{z}_1, \ldots, \boldsymbol{z}_H | \mathbf{a}, \sigma^2, H_0)} \underset{H_0}{\overset{H_1}{\gtrless}} T \qquad N \gg M, \tag{5}$$

where $\boldsymbol{\alpha} = [\alpha_1, \ldots, \alpha_H]$, $f(\boldsymbol{z}_1, \ldots, \boldsymbol{z}_H | \mathbf{a}, \sigma^2, \boldsymbol{\alpha}, H_0)$ and $f(\boldsymbol{z}_1, \ldots, \boldsymbol{z}_H | \mathbf{a}, \sigma^2, H_1)$ are the pdf's of the data vectors under H_0 and H_1 respectively. Moreover, exploiting the independence of the vectors $\boldsymbol{z}_t$, $t = 1, \ldots, H$, we can write the joint pdf's as

$$f(\boldsymbol{z}_1, \ldots, \boldsymbol{z}_H | \mathbf{a}, \sigma^2, H_0) = \frac{1}{(\pi\sigma^2)^{(N-M)H}} \exp\left\{-\frac{1}{\sigma^2} \sum_{t=1}^{H} (\boldsymbol{u}_t - \boldsymbol{Z}_t \mathbf{a})^\dagger (\boldsymbol{u}_t - \boldsymbol{Z}_t \mathbf{a})\right\} \tag{6}$$

$$f(\boldsymbol{z}_1, \ldots, \boldsymbol{z}_H | \mathbf{a}, \sigma^2, \boldsymbol{\alpha}, H_1) =$$

$$\frac{1}{(\pi\sigma^2)^{(N-M)H}} \exp\left\{-\frac{1}{\sigma^2} \sum_{t=1}^{H} (\boldsymbol{u}_t - \alpha_t \boldsymbol{q} - \boldsymbol{Z}_t \mathbf{a} - \alpha_t \boldsymbol{P}\mathbf{a})^\dagger (\boldsymbol{u}_t - \alpha_t \boldsymbol{q} - \boldsymbol{Z}_t \mathbf{a} - \alpha_t \boldsymbol{P}\mathbf{a})\right\} \tag{7}$$

It is now necessary to evaluate the maximum of (6) and (7) with respect to the unknown parameters. To this end we observe that in [14] it has been shown that

$$\max_{\sigma^2, \mathbf{a}} f(\boldsymbol{z}_1, \ldots, \boldsymbol{z}_H | \mathbf{a}, \sigma^2, H_0) = \left[\frac{(N-M)H}{\pi \sum_{t=1}^{H} (\boldsymbol{u}_t - \boldsymbol{Z}_t \widehat{\mathbf{a}_0})^\dagger (\boldsymbol{u}_t - \boldsymbol{Z}_t \widehat{\mathbf{a}_0})}\right]^{(N-M)H}, \tag{8}$$

where $\widehat{\mathbf{a}_0} = \left(\sum_{t=1}^{H} \boldsymbol{Z}_t^\dagger \boldsymbol{Z}_t\right)^{-1} \sum_{t=1}^{H} \boldsymbol{Z}_t^\dagger \boldsymbol{u}_t$.

Moreover maximizing (7) over σ^2 yields

$$\max_{\sigma^2} f(\boldsymbol{z}_1, \ldots, \boldsymbol{z}_H | \mathbf{a}, \sigma^2, \boldsymbol{\alpha}, H_1) =$$

$$\left[\frac{(N-M)H}{\pi \sum_{t=1}^{H} (\boldsymbol{u}_t - \alpha_t \boldsymbol{q} - \boldsymbol{Z}_t \mathbf{a} - \alpha_t \boldsymbol{P}\mathbf{a})^\dagger (\boldsymbol{u}_t - \alpha_t \boldsymbol{q} - \boldsymbol{Z}_t \mathbf{a} - \alpha_t \boldsymbol{P}\mathbf{a})}\right]^{(N-M)H}. \tag{9}$$

Maximizing the last quantity with respect to $\boldsymbol{\alpha}$ is tantamount to minimizing the quadratic forms

$$J(\alpha_t) = (\boldsymbol{u}_t - \alpha_t \boldsymbol{q} - \boldsymbol{Z}_t \mathbf{a} - \alpha_t \boldsymbol{P}\mathbf{a})^\dagger (\boldsymbol{u}_t - \alpha_t \boldsymbol{q} - \boldsymbol{Z}_t \mathbf{a} - \alpha_t \boldsymbol{P}\mathbf{a}) \tag{10}$$

over α_t, $t = 1, \ldots, H$. Hence, after some algebra, it can be shown that

$$\min_{\alpha_t} J(\alpha_t) = (\boldsymbol{u}_t - \boldsymbol{Z}_t \mathbf{a})^\dagger \boldsymbol{H} (\boldsymbol{u}_t - \boldsymbol{Z}_t \mathbf{a}) \tag{11}$$

where $\boldsymbol{H}$ is the projection matrix

$$\boldsymbol{I} - \frac{(\boldsymbol{q} + \boldsymbol{P}\mathbf{a})(\boldsymbol{q} + \boldsymbol{P}\mathbf{a})^\dagger}{(\boldsymbol{q} + \boldsymbol{P}\mathbf{a})^\dagger(\boldsymbol{q} + \boldsymbol{P}\mathbf{a})}. \tag{12}$$

Expression (11) implies that

$$\max_{\sigma^2, \boldsymbol{\alpha}} f(\boldsymbol{z}_1, \ldots, \boldsymbol{z}_H | \mathbf{a}, \sigma^2, \boldsymbol{\alpha}, H_1) = \left[\frac{(N-M)H}{\pi \sum_{t=1}^{H} (\boldsymbol{u}_t - \boldsymbol{Z}_t \mathbf{a})^\dagger \boldsymbol{H} (\boldsymbol{u}_t - \boldsymbol{Z}_t \mathbf{a})}\right]^{(N-M)H}. \tag{13}$$

It still remains to maximize the last expression over $\mathbf{a}$. To this end we note that in [19] it is shown that the matrix (12) is independent of $\mathbf{a}$ and can be written as $\boldsymbol{I} - \frac{\boldsymbol{\phi}\,\boldsymbol{\phi}^\dagger}{\boldsymbol{\phi}^\dagger\,\boldsymbol{\phi}}$ where $\boldsymbol{\phi} = [1, e^{j2\pi f_d}, \ldots, e^{j2\pi(N-M-1)f_d}]^T$. Thus maximizing (13) with respect to $\mathbf{a}$, after some algebraic manipulations, yields

$$\max_{\sigma^2, \boldsymbol{\alpha}, \mathbf{a}} f(\boldsymbol{z}_1, \ldots, \boldsymbol{z}_H | \mathbf{a}, \sigma^2, \boldsymbol{\alpha}, H_1) = \left[\frac{(N-M)H}{\pi \sum_{t=1}^{H} (\boldsymbol{u}_t - \boldsymbol{Z}_t \widehat{\mathbf{a}_1})^\dagger \boldsymbol{H} (\boldsymbol{u}_t - \boldsymbol{Z}_t \widehat{\mathbf{a}_1})}\right]^{(N-M)H}. \tag{14}$$

where $\widehat{\mathbf{a}_1} = \left(\sum_{t=1}^{H} \boldsymbol{Z}_t^\dagger \boldsymbol{H} \boldsymbol{Z}_t\right)^{-1} \sum_{t=1}^{H} \boldsymbol{Z}_t^\dagger \boldsymbol{H} \boldsymbol{u}_t$. Finally, working backward, we come up with the following decision rule

$$\frac{\sum_{t=1}^{H} (\boldsymbol{u}_t - \boldsymbol{Z}_t \widehat{\mathbf{a}_0})^\dagger (\boldsymbol{u}_t - \boldsymbol{Z}_t \widehat{\mathbf{a}_0})}{\sum_{t=1}^{H} (\boldsymbol{u}_t - \boldsymbol{Z}_t \widehat{\mathbf{a}_1})^\dagger \boldsymbol{H} (\boldsymbol{u}_t - \boldsymbol{Z}_t \widehat{\mathbf{a}_1})} \underset{H_0}{\overset{H_1}{\gtrless}} T_1, \tag{15}$$

where T_1 is the appropriate modification of the threshold in (5). We explicitly point out that the decision statistic performs a comparison between the estimates of σ^2 under the hypotheses H_0 and H_1. Moreover, due to the homogeneous assumption, the estimators exploit, through a non-coherent integration (summation), all the H available data vectors. However, under the H_1 hypothesis, the data are first projected into the null space of $\boldsymbol{\phi}$ in order to get target free observations. Remarkably the newly receiver (15) ensures the CFAR property with respect to σ^2. In fact, under the hypothesis H_0, this parameter factors out between the numerator and the denominator of (15).

It is worth pointing out that receiver (15) assumes the knowledge of the model order M or equivalently that a reliable estimate of M is available. However it is possible conceiving a more general version of the detector that gets rid of the quoted information. Precisely, denoting by M_0 the maximum of M over all the expected disturbance scenarios (as previously pointed out $M_0 = 5$ for radar scenarios and $M_0 = 8$ for the sonar case

[14]), the methodology adopted to cope with a possible uncertainty about M could be that of evaluating the GLRT over the model order with the constraint $M \in (1, \ldots, M_0)$. Otherwise stated it is reasonable considering the following decision rule

$$\frac{\max\limits_{M\in(1,\ldots,M_0)} \max\limits_{\sigma^2,\, \boldsymbol{\alpha},\mathbf{a}} f(\, \boldsymbol{z}_1, \ldots,\, \boldsymbol{z}_H | M, \mathbf{a}, \sigma^2,\, \boldsymbol{\alpha}, H_1)}{\max\limits_{M\in(1,\ldots,M_0)} \max\limits_{\sigma^2,\mathbf{a}} f(\, \boldsymbol{z}_1, \ldots,\, \boldsymbol{z}_H | M, \mathbf{a}, \sigma^2, H_0)} \underset{H_0}{\overset{H_1}{\gtrless}} T \qquad N \gg M, \tag{16}$$

which, exploiting (13) and (14), can be recast as

$$\frac{\min\limits_{M\in(1,\ldots,M_0)} \sum_{t=1}^{H} (\, \boldsymbol{u}_t - \, \boldsymbol{Z}_t \widehat{\mathbf{a}_0})^\dagger (\, \boldsymbol{u}_t - \, \boldsymbol{Z}_t \widehat{\mathbf{a}_0})}{\min\limits_{M\in(1,\ldots,M_0)} \sum_{t=1}^{H} (\, \boldsymbol{u}_t - \, \boldsymbol{Z}_t \widehat{\mathbf{a}_1})^\dagger \, \boldsymbol{H} (\, \boldsymbol{u}_t - \, \boldsymbol{Z}_t \widehat{\mathbf{a}_1})} \underset{H_0}{\overset{H_1}{\gtrless}} T_1 . \tag{17}$$

Notice that the minimization over M is to be performed through an exhaustive search over the discrete set $(1, \ldots, M_0)$ leading to an increase in the computational complexity with respect to the case of known M. Finally receiver (17) still ensures the CFAR property with respect to the parameter σ^2.

2.2 Heterogeneous Environment

In this case each data vector possesses a different covariance matrix. Thus the AGLRT can be written as

$$\frac{\max_{\boldsymbol{\sigma},\, \boldsymbol{\alpha},\, \boldsymbol{A}} f(\, \boldsymbol{z}_1, \ldots,\, \boldsymbol{z}_H |\, \boldsymbol{A},\, \boldsymbol{\sigma},\, \boldsymbol{\alpha}, H_1)}{\max_{\boldsymbol{\sigma},\, \boldsymbol{A}} f(\, \boldsymbol{z}_1, \ldots,\, \boldsymbol{z}_H |\, \boldsymbol{A},\, \boldsymbol{\sigma}, H_0)} \underset{H_0}{\overset{H_1}{\gtrless}} G \qquad N \gg M, \tag{18}$$

where $\boldsymbol{A} = [\mathbf{a}_1, \ldots, \mathbf{a}_H]$, $\boldsymbol{\sigma} = [\sigma_1^2, \ldots, \sigma_H^2]^T$ and the joint pdf's of $\boldsymbol{z}_1, \ldots,\, \boldsymbol{z}_H$ are

$$f(\, \boldsymbol{z}_1, \ldots,\, \boldsymbol{z}_H |\, \boldsymbol{A},\, \boldsymbol{\sigma}, H_0) = \prod_{t=1}^{H} f(\, \boldsymbol{z}_t | \mathbf{a}_t, \sigma_t^2, H_0) \tag{19}$$

and

$$f(\, \boldsymbol{z}_1, \ldots,\, \boldsymbol{z}_H |\, \boldsymbol{A},\, \boldsymbol{\sigma},\, \boldsymbol{\alpha}, H_1) = \prod_{t=1}^{H} f(\, \boldsymbol{z}_t | \mathbf{a}_t, \sigma_t^2, \alpha_t, H_1) \tag{20}$$

under H_0 and H_1 respectively. To perform the maximizations required in (18) we observe that

$$\max_{\boldsymbol{\sigma},\, \boldsymbol{A}} f(\, \boldsymbol{z}_1, \ldots,\, \boldsymbol{z}_H |\, \boldsymbol{A},\, \boldsymbol{\sigma}, H_0) = \prod_{t=1}^{H} \max_{\sigma_t^2, \mathbf{a}_t} f(\, \boldsymbol{z}_t | \mathbf{a}_t, \sigma_t^2, H_0) \tag{21}$$

$$\max_{\boldsymbol{\sigma},\,\boldsymbol{\alpha},\,\boldsymbol{A}} f(\boldsymbol{z}_1,\ldots,\,\boldsymbol{z}_H|\,\boldsymbol{A},\,\boldsymbol{\sigma},\,\boldsymbol{\alpha},H_1) = \prod_{t=1}^{H} \max_{\sigma_t^2,\alpha_t,\mathbf{a}_t} f(\boldsymbol{z}_t|\mathbf{a}_t,\sigma_t^2,\alpha_t,H_1) \tag{22}$$

Moreover, from (8) and (14) it follows that

$$\max_{\sigma_t^2,\mathbf{a}_t} f(\boldsymbol{z}_t|\mathbf{a}_t,\sigma_t^2,H_0) = \left[\frac{(N-M)}{\pi(\boldsymbol{u}_t - \boldsymbol{Z}_t\widehat{\mathbf{a}_{t,0}})^\dagger(\boldsymbol{u}_t - \boldsymbol{Z}_t\widehat{\mathbf{a}_{t,0}})}\right]^{(N-M)}, \tag{23}$$

$$\max_{\sigma_t^2,\alpha_t,\mathbf{a}_t} f(\boldsymbol{z}_t|\mathbf{a}_t,\sigma_t^2,\alpha_t,H_1) = \left[\frac{(N-M)}{\pi(\boldsymbol{u}_t - \boldsymbol{Z}_t\widehat{\mathbf{a}_{t,1}})^\dagger\,\boldsymbol{H}(\boldsymbol{u}_t - \boldsymbol{Z}_t\widehat{\mathbf{a}_{t,1}})}\right]^{(N-M)}, \tag{24}$$

where $\widehat{\mathbf{a}_{t,0}} = \left(\boldsymbol{Z}_t^\dagger\,\boldsymbol{Z}_t\right)^{-1}\,\boldsymbol{Z}_t^\dagger\,\boldsymbol{u}_t$ and $\widehat{\mathbf{a}_{t,1}} = \left(\boldsymbol{Z}_t^\dagger\,\boldsymbol{H}\,\boldsymbol{Z}_t\right)^{-1}\,\boldsymbol{Z}_t^\dagger\,\boldsymbol{H}\,\boldsymbol{u}_t$. Finally, substituting (23) in (21) and (24) in (22) we can rewrite the AGLRT (18) as

$$\prod_{t=1}^{H}\frac{(\boldsymbol{u}_t - \boldsymbol{Z}_t\widehat{\mathbf{a}_{t,0}})^\dagger(\boldsymbol{u}_t - \boldsymbol{Z}_t\widehat{\mathbf{a}_{t,0}})}{(\boldsymbol{u}_t - \boldsymbol{Z}_t\widehat{\mathbf{a}_{t,1}})^\dagger\,\boldsymbol{H}(\boldsymbol{u}_t - \boldsymbol{Z}_t\widehat{\mathbf{a}_{t,1}})} \underset{H_0}{\overset{H_1}{\gtrless}} G_1\,, \tag{25}$$

where G_1 is the appropriate modification of the threshold in (18). The decision statistic compares the geometric mean of the σ_t^2's estimates under H_0, with the geometric mean of the σ_t^2's estimates under H_1. Moreover, as in the homogeneous case, the data exploited under H_1 are first projected into the null space of $\boldsymbol{\phi}$ in order to get target free observations. Interestingly receiver (18) ensures the CFAR property with respect to σ_t^2, $t = 1,\ldots,H$.

As in Subsection 2.1 it is possible generalizing receiver (25) accounting for a partial uncertainty on the model order M. Otherwise stated one can consider the following decision rule

$$\frac{\max\limits_{M\in(1,\ldots,M_0)}\ \max\limits_{\boldsymbol{\sigma},\,\boldsymbol{\alpha},\,\boldsymbol{A}} f(\boldsymbol{z}_1,\ldots,\,\boldsymbol{z}_H|M,\,\boldsymbol{A},\,\boldsymbol{\sigma},\,\boldsymbol{\alpha},H_1)}{\max\limits_{M\in(1,\ldots,M_0)}\ \max\limits_{\boldsymbol{\sigma},\,\boldsymbol{A}} f(\boldsymbol{z}_1,\ldots,\,\boldsymbol{z}_H|M,\,\boldsymbol{A},\,\boldsymbol{\sigma},H_0)} \underset{H_0}{\overset{H_1}{\gtrless}} G \qquad N \gg M, \tag{26}$$

which, after some algebraic manipulations exploiting also (23) and (24), can be rewritten as

$$\frac{\min\limits_{M\in(1,\ldots,M_0)} \prod_{t=1}^{H}(\boldsymbol{u}_t - \boldsymbol{Z}_t\widehat{\mathbf{a}_{t,0}})^\dagger(\boldsymbol{u}_t - \boldsymbol{Z}_t\widehat{\mathbf{a}_{t,0}})}{\min\limits_{M\in(1,\ldots,M_0)} \prod_{t=1}^{H}(\boldsymbol{u}_t - \boldsymbol{Z}_t\widehat{\mathbf{a}_{t,1}})^\dagger\,\boldsymbol{H}(\boldsymbol{u}_t - \boldsymbol{Z}_t\widehat{\mathbf{a}_{t,1}})} \underset{H_0}{\overset{H_1}{\gtrless}} G_1\,. \tag{27}$$

Notice that the CFAR property with respect to σ_t^2, $t = 1,\ldots,H$ still holds. Finally, if $H = 1$ namely point-like target, detector (15) coincides with (25) whereas detector (17) coincides with (27).

3 Performance Assessment

In this section we assess the performance of the detectors (15), (17), (25), and (27) in terms of the probability of false alarm (P_{fa}) and the probability of detection (P_d). To this end, we first note that closed form expressions for both (P_{fa}) as well as (P_d) are not available, but for the asymptotic case, i.e. when N tends to infinity, and the receivers (15) and (25).

Specifically, it can be shown that for $N \to \infty$ and under H_0 the GLRT's (15) and (25) are distributed according to a central chi square random variable with $2H$ degrees of freedom [27]. Thus, the asymptotic expression for the P_{fa} is

$$P_{fa} = e^{-\frac{G}{2}} \sum_{j=0}^{H-1} \frac{1}{j!} \left(\frac{G}{2} \right)^j , \tag{28}$$

which highlights that the proposed decision rules are asymptotically CFAR with respect to the covariance matrix.

As to the asymptotic P_d we notice that, under H_1 and for $N \to \infty$, the GLRT's (15) and (25) are distributed according to a non-central chi square random variables with $2H$ degrees of freedom and non-centrality parameters

$$\lambda = \begin{cases} 2\sum_{t=1}^{H} |\alpha_t|^2 \, \boldsymbol{p}^\dagger \, \boldsymbol{R}^{-1} \, \boldsymbol{p} & \text{receiver (15)} \\ 2\sum_{t=1}^{H} |\alpha_t|^2 \, \boldsymbol{p}^\dagger \, \boldsymbol{R}_t^{-1} \, \boldsymbol{p} & \text{receiver (25)} \end{cases} \tag{29}$$

where $\boldsymbol{R}$ ($\boldsymbol{R}_t$) is the covariance matrix of the disturbance vector $\mathbf{n}_t$, $t = 1, \ldots, H$, with reference to the homogeneous (heterogeneous) scenario (see Appendix 1 for the proof). It follows that the P_d can be expressed as

$$P_d = \mathcal{Q}_H \left(\sqrt{\lambda}, \sqrt{G} \right) , \tag{30}$$

where $\mathcal{Q}_H(\cdot,\cdot)$ denotes the Marcum function [28]. The above expression also shows that the asymptotic performance is irrespective of the statistical characterization of the α_t's phase. Indeed it can be shown that this is a general performance trend, namely it holds true even for finite values of N.

In this last case, however, we must numerically evaluate the performance of all the proposed receivers. To this end we resort to Monte Carlo techniques, based on $\dfrac{100}{P_{fa}}$ and

$\frac{100}{P_d}$ independent trials, for P_{fa} and for P_d, respectively. Moreover, in order to limit the computational burden, we assume $P_{fa} = 10^{-4}$. Further developments require specifying both the disturbance as well as the target model.

Disturbance Model. As previously stated, the clutter is modeled as an AR Gaussian process of order M and parameters $\mathbf{a}$ and σ^2 for the homogeneous case, and $\mathbf{a}_1, \ldots, \mathbf{a}_H$, $\sigma_1^2, \ldots, \sigma_H^2$ with reference to the heterogeneous environment. In order to evaluate the performance it is necessary assigning both the order of the clutter process as well as the values of the unknown parameters. We carry out order selection and parameters estimation analyzing the spectral properties of the data collected by the McMaster IPIX radar in Grimsby, on the shore of Lake Ontario, in winter 1998 [29]. The quoted system is a fully coherent X-band radar, with advanced features such as dual transmit/receive polarization, frequency agility, and stare/surveillance mode. We refer to the dataset *file_19980223_170435_antstep.cdf*, range resolution 15m and in particular to the range cells from the 11-th to the 20-th. A thorough statistical analysis of the aforementioned dataset has been conducted in [30] and the results have highlighted the compatibility of the data with the SIRP model.

Our first goal is to proper select the model order. It is well known that many problems may arise in estimating the order of an AR process, in particular when the sample size N is smaller than $10P$, where P denotes the maximum possible value of the process order. Several studies have been carried out on this topic [31, and references therein], leading to different selection criteria whose common starting point is the minimization of a function involving the Kullback-Leibler discrepancy [32]. An extensive discussion on the performance and the applicability of those criteria is reported in [31].

In this work order selection is achieved by fitting the non-parametric estimate of the clutter PSD, performed by means the Welch method [33], with the AR PSD of increasing order starting from $M = 1$. As to the method employed for estimating the unknown AR parameters, we resort to the Burg technique [26]. Indeed recent comparisons between the various approaches, proposed in the last decades for estimating the AR parameters, have shown that the Burg technique guarantees stationarity of the estimated model ensuring also a small bias and a small finite sample variance.

Cell Number	Disturbance Parameters			
	$a_t(1)$	$a_t(2)$	$a_t(3)$	σ_t^2
1	0.85 - 0.52i	0.02 - 0.19i	0.09 + 0.26i	35.907
2	0.45 - 0.29i	0.09 - 0.26i	-0.01 - 0.05i	46.673
3	0.46 - 0.21i	0.17 - 0.20i	0.01 - 0.06i	50.604
4	0.47 - 0.26i	0.12 - 0.22i	0.01 - 0.03i	52.13
5	0.74 - 0.51i	0.06 - 0.20i	0.07 - 0.23i	42.23
6	0.59 - 0.35i	0.11 - 0.25i	-0.01 + 0.07i	43.51
7	0.63 - 0.40i	0.10 - 0.24i	0.01 + 0.12i	45.81
8	0.62 - 0.37i	0.10 - 0.23i	0.01 + 0.16i	42.05
9	-0.64 + 0.36i	-0.14 + 0.23i	-0.02 - 0.19i	40.99
10	-0.46 + 0.24i	-0.13 + 0.22i	0.01 + 0.04i	51.46

Table I: AR parameters of the clutter process. Order $M = 3$. Cells from 11-th to 20-th, dataset *file_19980223_170435_antstep.cdf*, HH polarimetric channel.

The results of the spectral analysis show that a good match between the parametric and the non-parametric estimate of the PSD is obtained modeling the disturbance as an AR process of order 3. In particular, in Figure 1, we compare the estimated power spectrum of the returns from the 13-th range cell of the dataset performed exploiting the Welch method with the parametric AR PSD employing the Burg technique. The plots, which refer to both the co-polarized HH and VV as well as to the cross-polarized HV and VH channels, confirm that $M = 3$ is adequate for a good fitting. Finally, in Table I, we report the estimates of the AR parameters, with reference to the range cells from the 11-th to the 20-th of the real dataset and the HH polarimetric channel, which will be used in the rest of the paper for simulation purposes.

Target Model. We adopt a deterministic multiple dominant scatterers (MDS) model with $H = 10$ and the target scatterers' locations given in Table II: for each cell we indicate the percentage of total useful target energy backscattered from that cell. As to the total energy from the target, $\mathcal{E}$ say, it is the sum of the energies, $\mathcal{E}_t = |\alpha_t|^2 \mathbf{p}^\dagger \mathbf{p}$, $t = 1, \ldots, H$, say, from the target scatterers, i.e.,

$$\mathcal{E} = \sum_{t=1}^{H} \mathcal{E}_t \, .$$

Notice that a more general target model accounting also for a possible fluctuation as well

Model Number	Cell Number									
	1	2	3	4	5	6	7	8	9	10
M_1	1/10	1/10	1/10	1/10	1/10	1/10	1/10	1/10	1/10	1/10
M_2	2/5	3/10	1/5	1/10	0	0	0	0	0	0
M_3	3/4	1/4	0	0	0	0	0	0	0	0

Table II: Target models with $H = 10$, discrete scatterers' locations and percentage of total energy reflected, i.e., $\frac{\mathcal{E}_t}{\mathcal{E}}$, $t = 1, \ldots, H$.

as a possible correlation of the amplitudes α_t's can be found in [6].

Simulation Results. In the following we plot the performance of the detectors (15), (17), (25), and (27) in terms of P_d, versus the SCR, defined as

$$SCR = \begin{cases} 2\sum_{t=1}^{H} |\alpha_t|^2 \, \boldsymbol{p}^\dagger \, \boldsymbol{R}^{-1} \, \boldsymbol{p} & \text{receivers (15) and (17)} \\ 2\sum_{t=1}^{H} |\alpha_t|^2 \, \boldsymbol{p}^\dagger \, \boldsymbol{R}_t^{-1} \, \boldsymbol{p} & \text{receivers (25) and (27)} \end{cases}$$

Notice that real radar data have been only exploited for estimating the model order, the AR parameters, and thus, via the algorithm of [34, 26], the covariance matrix of the disturbance process. However both P_{fa} and P_d have been obtained by means of data simulated according to the models described in Section 2. Otherwise stated $\mathbf{n}_t$'s, $t = 1, \ldots, H$, are independent complex AR Gaussian vectors whose model order and parameters coincide with the values estimated from the real dataset. Precisely, the model order has been selected equal to 3. Moreover, with reference to the homogeneous environment, the AR parameters have been chosen as the average of the values reported in each column of Table I, whereas for the heterogeneous environment they are just the values displayed in each column of the table.

In Figure 2 we plot the performance of the detectors (15) and (17) for $P_{fa} = 10^{-4}$, $f_d = 0.03$, $H = 10$, $M = 3$, $M_0 = 6$, and several values of N. Moreover, for comparison purposes, the asymptotic performance is displayed too. The curves show that the performance loss with respect to the asymptotic case, defined as the horizontal displacement of the corresponding curves, is kept within 3 dB for $N = 40$, $P_d = 0.9$ and both the detectors. The trends of the curves also highlight that receiver (15) converges more quickly than detector (17). In fact the former achieves almost the same detection performance for $N = 30$ and $N = 40$ whereas the latter shows a performance improvement when the sample size ranges from $N = 30$ to $N = 40$. Finally, notice also that, for the homogeneous case, the performance is irrespective of the actual MDS target model.

In Figures 3a, 3b, and 3c we consider the case of heterogeneous environment. Specifically, we plot the performance of the detectors (25) and (27), for $P_{fa} = 10^{-4}$, $f_d = 0.03$, $H = 10$, $M = 3$, $M_0 = 6$, several values of N, and the target models of Table II. In particular, Figure 3a refers to the target model M_1 whereas Figures 3b and 3c to the models M_2 and M_3, respectively. The curves still show that an increase in the sample size leads to better and better performances. Moreover the loss with respect to the asymptotic curve strongly depends on the target model being in force. In particular, the more concentrated the target, the poorer the performance. Otherwise stated the receivers suffer a collapsing loss.

We also highlight that the sample size required to ensure satisfactory performances is greater than the value required for the homogeneous case. This behavior can be easily explained observing that in the case at hand the size of the parameter space is larger and thus a greater sample size is required for achieving reliable parameter estimates. Before concluding we notice that for $N < 50$ the receiver (27) which does not assume the knowlwdge of M suffers a heavier performance loss with respect to the receiver (25) which knows M. Finally this loss can be partially compensated increasing N.

4 Conclusions

In this paper we have considered the design and the analysis of radar detectors for range-spread targets embedded in Gaussian disturbance modeled as an AR process of order M. We have focused on two distinct scenarios (the homogeneous and the heterogeneous environments) and for each of them we have devised two detectors. The former receiver assumes the perfect knowledge of the model order M whereas the latter gets rid of this *a-priori* information. Both ensure the CFAR property with respect to the disturbance power levels and one of them is also asymptotically CFAR with respect to the disturbance covariance matrix.

At the analysis stage we have evaluated the performance of the newly introduced detectors in terms of P_{fa} and P_d. To this end we have first performed a spectral analysis on real radar clutter collected by the IPIX Radar in 1998 in order to estimate the actual AR parameters as well as the model order to be used in the simulations. Thus we have analyzed the behavior of the novel detectors for $P_{fa} = 10^{-4}$. The results have shown that they achieve in general satisfactory performances. Moreover the P_d of the receivers designed in the presence of homogeneous environment is irrespective of the actual target model. On the contrary detectors designed for the heterogeneous scenario suffer the collapsing loss namely the more concentrated the target, the poorer the performance.

Before concluding we highlight that assuming the presence of secondary data (free of useful target signal) the number of Doppler samples N, required to achieve a given performance level, reduces. Otherwise stated it is possible to trade off Doppler samples with secondary data.

Finally, a possible future research track could concern the extension of the approach to the multichannel case.

Acknowledgments

The authors are deeply in debt to Prof. S. Haykin and Dr. B. Currie who have kindly provided the IPIX data.

5 Appendix 1

In this Appendix we derive the asymptotic expressions of the P_{fa} and the P_d for the receivers (15) and (25). To this end we denote with

- $Re(\cdot)$ and $Im(\cdot)$ the real and the imaginary parts of the argument, respectively;
- $\boldsymbol{\theta}_r = [Re(\alpha_1), Im(\alpha_1), \ldots, Re(\alpha_H), Im(\alpha_H)]^T$;
- $$\boldsymbol{\theta}_s = \begin{cases} [Re(\mathbf{a}^T), Im(\mathbf{a}^T), \sigma^2]^T & \text{receiver (15)} \\ [Re(\mathbf{a}_1^T), Im(\mathbf{a}_1^T), \ldots, Re(\mathbf{a}_H^T), Im(\mathbf{a}_H^T), \sigma_1^2, \ldots, \sigma_H^2]^T & \text{receiver (25)} \end{cases}$$
- $\boldsymbol{\theta} = [\ \boldsymbol{\theta}_r^T,\ \boldsymbol{\theta}_s^T]^T$;

- $\boldsymbol{J}(\boldsymbol{\theta}) = \boldsymbol{J}(\boldsymbol{\theta}_r, \boldsymbol{\theta}_s)$ the Fisher information matrix [35] which can be partitioned as

$$\boldsymbol{J}(\boldsymbol{\theta}) = \begin{bmatrix} \boldsymbol{J}_{\boldsymbol{\theta}_r, \boldsymbol{\theta}_r}(\boldsymbol{\theta}) & \boldsymbol{J}_{\boldsymbol{\theta}_r, \boldsymbol{\theta}_s}(\boldsymbol{\theta}) \\ \boldsymbol{J}_{\boldsymbol{\theta}_s, \boldsymbol{\theta}_r}(\boldsymbol{\theta}) & \boldsymbol{J}_{\boldsymbol{\theta}_s, \boldsymbol{\theta}_s}(\boldsymbol{\theta}) \end{bmatrix}.$$

According to [27], under H_0 and for $N \to \infty$, the GLRT is distributed according to a central chi square random variable with $2H$ degrees of freedom. Hence, exploiting [28, pp. 1 formula B3], we get (28). Moreover, under H_1 and for $N \to \infty$, the GLRT follows a non-central chi square random variable with $2H$ degrees of freedom and non-centrality parameter

$$\lambda = \boldsymbol{\theta}_r^T \left[\boldsymbol{J}_{\boldsymbol{\theta}_r, \boldsymbol{\theta}_r}(\boldsymbol{\theta}) - \boldsymbol{J}_{\boldsymbol{\theta}_r, \boldsymbol{\theta}_s}(\boldsymbol{\theta}) \boldsymbol{J}^{-1}_{\boldsymbol{\theta}_s, \boldsymbol{\theta}_s}(\boldsymbol{\theta}) \boldsymbol{J}_{\boldsymbol{\theta}_s, \boldsymbol{\theta}_r}(\boldsymbol{\theta}) \right] \Big|_{\boldsymbol{\theta} = [\,\mathbf{0}_{1,2H},\, \boldsymbol{\theta}_s^T]} \boldsymbol{\theta}_r,$$

where $\mathbf{0}_{m,n}$ denotes a $m \times n$ matrix of zeros. Hence, exploiting [28, pp. 2 formula C3], we get the asymptotic P_d (30).

Further developments require evaluating the Fisher information matrices for both the receivers (15) and (25). As to the former it can be shown, after some algebra, that

$$\begin{aligned} \boldsymbol{J}_{\boldsymbol{\theta}_r, \boldsymbol{\theta}_r}(\boldsymbol{\theta}) &= 2\mathrm{p}^\dagger \boldsymbol{R}^{-1} \mathrm{p}\, \boldsymbol{I}_{2H} \\ \boldsymbol{J}_{\boldsymbol{\theta}_r, \boldsymbol{\theta}_s}(\boldsymbol{\theta}) &= \boldsymbol{J}^T_{\boldsymbol{\theta}_r, \boldsymbol{\theta}_s}(\boldsymbol{\theta}) = \mathbf{0}_{2H,2M+1}; \end{aligned} \tag{31}$$

where $\boldsymbol{I}_m$ is the $m \times m$ identity matrix. Thus, substituting (31) in (5) we can recast the non-centrality parameter as

$$\lambda = 2 \sum_{t=1}^{H} |\alpha_t|^2\, \boldsymbol{p}^\dagger \boldsymbol{R}^{-1} \boldsymbol{p}.$$

As to the latter it can be proved, after some algebra, that

$$\begin{aligned} \boldsymbol{J}_{\boldsymbol{\theta}_r, \boldsymbol{\theta}_r}(\boldsymbol{\theta}) &= 2\ diag(\mathrm{p}^\dagger \boldsymbol{R}_1^{-1}\mathrm{p}, \ldots, \mathrm{p}^\dagger \boldsymbol{R}_H^{-1}\mathrm{p}) \otimes \boldsymbol{I}_2 \\ \boldsymbol{J}_{\boldsymbol{\theta}_r, \boldsymbol{\theta}_s}(\boldsymbol{\theta}) &= \boldsymbol{J}^T_{\boldsymbol{\theta}_r, \boldsymbol{\theta}_s}(\boldsymbol{\theta}) = \mathbf{0}_{2H,(2M+1)H} \end{aligned} \tag{32}$$

where $diag(\delta_1, \ldots, \delta_{2H})$ denotes a diagonal matrix with diagonal elements $\delta_1, \ldots, \delta_{2H}$ and $\otimes$ the Kronecker product. Hence substituting (32) in (5) we get the non-centrality parameter, i.e.

$$\lambda = 2 \sum_{t=1}^{H} |\alpha_t|^2\, \boldsymbol{p}^\dagger \boldsymbol{R}_t^{-1} \boldsymbol{p}.$$

References

[1] H. L. Van Trees: *Detection, Estimation, and Modulation Theory*, John Wiley & Sons, 1968.

[2] A. Farina, F. Scannapieco, and F. Vinelli: "Target Detection and Classification with Very High Range Resolution Radar," *Proc. of International Conference on Radar*, Versailles, France, pp. 20-25, April 1989.

[3] A. Farina, F. Scannapieco, and F. Vinelli: "Target Detection and Classification with Polarimetric High Resolution Range Radar," *Direct and Inverse Methods in Radar Polarimetry*, W. M. Boerner Ed., Part. I, pp. 1021-1041, Klever Academic Publishers. Printed in Holland.

[4] T. T. Moon and P. J. Bawden: "High Resolution RCS Measurements of Boats," *IEE Proceedings-F*, vol. 138, No. 3, pp. 218-222, June 1991.

[5] K. Gerlach and M. J. Steiner: "Adaptive Detection of Range Distributed Targets," *IEEE Trans. on Signal Processing*, Vol. 47, No. 7, pp. 1844-1851, July 1999.

[6] E. Conte, A. De Maio, and G. Ricci: "GLRT-based Adaptive Detection Algorithms for Range-Spread Targets," *IEEE Trans. on Signal Processing*, Vol. 49, No. 7, pp. 1336-1348, July 2001.

[7] B. Himed and W. L. Melvin: "Analyzing Space-Time Adaptive Processors Using Measured Data," *Proc. of the Thirty-First Asilomar Conference on Signals, Systems & Computers*, pp. 930-935, 1998.

[8] R. S. Blum and K. F. McDonald: "Analysis of STAP Algorithms for Cases with Mismatched Steering and Clutter Statistics," *IEEE Trans. on Signal Processing*, Vol. 48, No. 2, pp. 301-310, February 2000.

[9] C. D. Richmond: "Performance of a Class of Adaptive Detection Algorithms in Nonhomogeneous Environments," *IEEE Trans. on Signal Processing*, Vol. 48, No. 5, pp. 1248-1262, May 2000.

[10] W. L. Melvin: "Space-Time Adaptive Radar Performance in Heterogeneous Clutter," *IEEE Trans. on Aerospace and Electronic Systems*, Vol. 36, No. 2, pp. 621-633, April 2000.

[11] W. L. Melvin, M. Wicks, P. Antonik, Y. Salama, P. Li, and H. Schuman: "Knowledge-Based Space-Time Adaptive Processing for Airborne Early Warning Radar," *IEEE AES Systems Magazine*, pp. 37-42, April 1998.

[12] D. J. Rabideau and A. O. Steinhardt: "Improved Adaptive Clutter Cancellation through Data-Adaptive Training," *IEEE Trans. on Aerospace and Electronic Systems*, Vol. 35, No. 3, pp. 879-891, July 1999.

[13] K. Gerlach and M. J. Steiner: "Fast Converging Adaptive Detection of Doppler-Shifted Range-Distributed Targets," *IEEE Trans. on Signal Processing*, Vol. 48, No. 9, pp. 2686-2690, September 2000.

[14] S. Haykin and A. Steinhardt: *Adaptive Radar Detection and Estimation*, Wiley, New York, 1992.

[15] J.H. Sawyers: "Adaptive Pulse-Doppler Radar Signal Processing using the Maximum Entropy Method," *Proc. of the EASCON 1980*, pp. 454-461, October 1980.

[16] E. D'Addio, A. Farina, F.A. Studer: "The Maximum Entropy Method and its Application to Clutter Cancellation," *Rivista Tecnica Selenia*, Vol.8, No.3, pp. 15-24, 1983.

[17] D. E. Bowyer, P. K. Rajasekaran, and W. W. Gebhart: "Adaptive Clutter Filtering Using Autoregressive Spectral Estimation," *IEEE Trans. on Aerospace and Electronic Systems*, Vol. 15, No. 4, pp. 538-546, July 1979.

[18] S. M. Kay: "Asymptotical Optimal Detection in Unknown Colored Noise Via Autoregressive Modeling," *IEEE Trans. on Acoustic Speech and Signal Processing*, Vol. 31, No. 4, pp. 927-940, August 1983.

[19] A. Sheikhi, M. M. Nayebi, M. R. Aref: "Adaptive Detection Algorithm for Radar Signals in Autoregressive Interference" IEE Proc.-Radar, Sonar Navig., Vol. 145, No. 5, pp. 309-314, October 1998

[20] J. R. Roman, M. Rangaswamy, D. W. Davis, Q. Zhang, B. Himed, and J. H. Michels: "Parametric Adaptive Matched Filter for Airborne Radar Applications," *IEEE Trans. on Aerospace and Electronic Systems*, Vol. 36, No. 2, pp. 677-692, April 2000.

[21] A. L. Swindlehurst, P. Stoica: "Maximum Likelihood Methods in Array Signal Processing," *Proceedings of the IEEE*, Vol. 8, No. 2, pp. 421-441, February 1998.

[22] J.H. Michels, B. Himed and M. Rangaswamy: "Performance of STAP Tests in Gaussian and Compound-Gaussian Clutter," *Digital Signal Processing*, Vol. 10, No. 4, pp. 309-324, October 2000.

[23] K. Gerlach: "Spatially Distributed Targets Detection in Non-Gaussian Clutter," *IEEE Trans. on Aerospace and Electronic Systems*, Vol. 35, No. 3, pp. 926-934, July 1999.

[24] E. Conte, M. Longo: "Characterisation of Radar Clutter as a Spherically Invariant Random Process," *IEE Proc.* Pt. F, Vol. 134, No. 2, pp. 191-197, April 1987.

[25] M. Rangaswamy, D. Weiner, and A. Ozturk: "Computer Generation of Correlated non-Gaussian Radar Clutter," *IEEE Trans. on Aerospace and Electronic Systems*, Vol. 31, No. 1, pp. 106 -116, January 1995.

[26] S. M. Kay: *Modern Spectral Estimation: Theory & Application*, Prentice-Hall, New Jersey, USA, 1988.

[27] S. M. Kay: *Fundamentals of Statistical Signal Processing: Detection Theory*, Prentice-Hall, New Jersey, USA, 1998.

[28] J. Omura and T. Kailath: "Some Useful Probability Distributions," *Technical Report No. 7050-6*, Systems Theory Laboratory, Stanford Electronics Laboratories, Stanford University, Stanford (CA), USA, 1965.

[29] http://soma.crl.mcmaster.ca/ipix/

[30] E. Conte, A. De Maio, and C. Galdi: "Statistical Analysis of Real Clutter at Different Range Resolutions," submitted for publication on *IEEE Trans. on Aerospace and Electronic Systems.*

[31] P.M.T. Broersen: "Finite Sample Criteria for Autoregressive Order Selection," *IEEE Trans. on Signal Processing*, Vol. 48, No. 12, pp. 3550-3558, December 2000.

[32] S.de Wale, P.M.T. Broersen: "Adaptive Detection with Time Series Models," *Proc. IEE Radar 2002*, pp. 449-453, Edinburgh, 15-17 October 2002.

[33] J.Proakis and D. G. Manolakis: *Digital Signal Processing*, Second Edition, Macmillan, USA, 1992.

[34] T. Kailath, A. Vieira, and M. Morf: "Inverse of Toeplitz Operators, Innovations, and Orthogonal Polynomials," *SIAM Rev.*, No. 20, pp. 106-119, 1978.

[35] L. L. Scharf: *Statistical Signal Processing. Detection, Estimation, and Time Series Analysis*, Addison-Wesley, 1991.

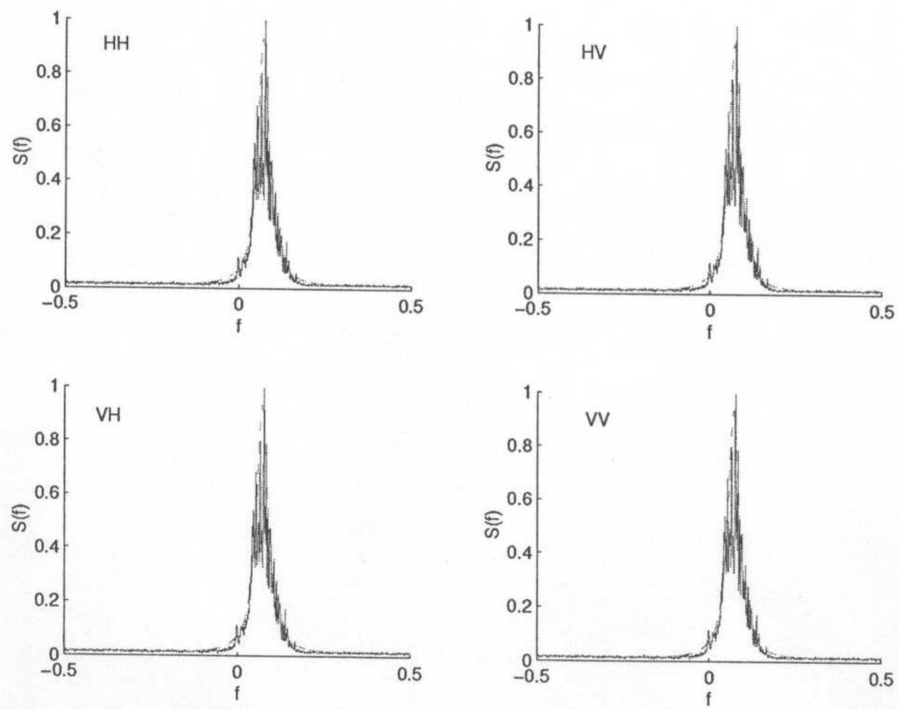

Figure 1. Power Spectral Density of the returns from the 13-th range cell versus the normalized frequency f. Model-based PSD estimates (dashed curves), non-parametric PSD estimates (solid curves).

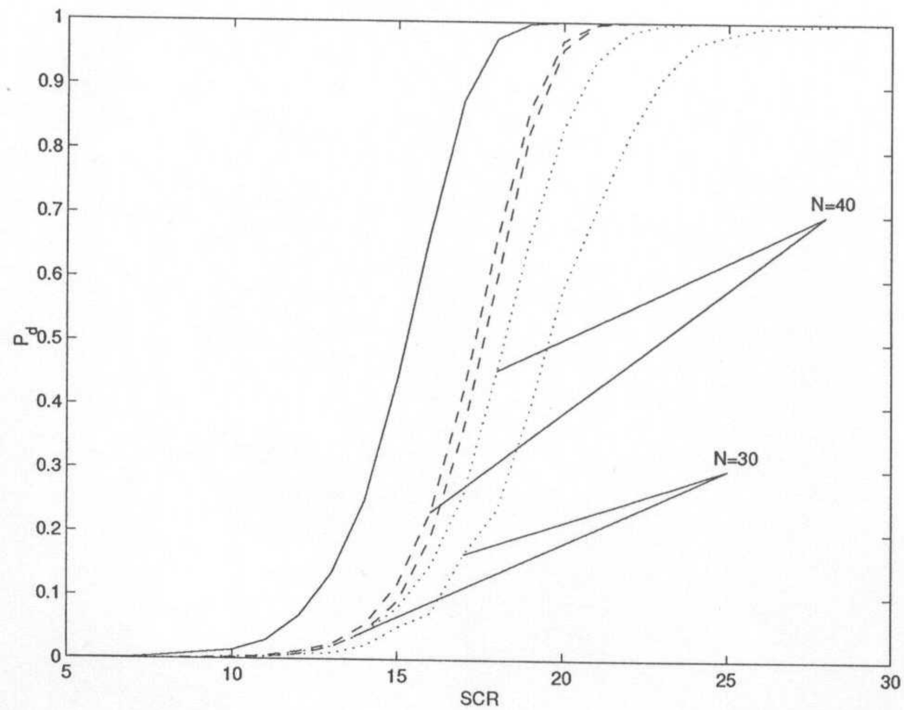

Figure 2. P_d versus SCR of the receiver (15) (dashed curve), (17) (dotted curve), and asymptotic performance $N = \infty$ (solid curve), for $P_{fa} = 10^{-4}$, $f_d = 0.03$, $H = 10$, $M = 3$, $M_0 = 6$, and N as a parameter.

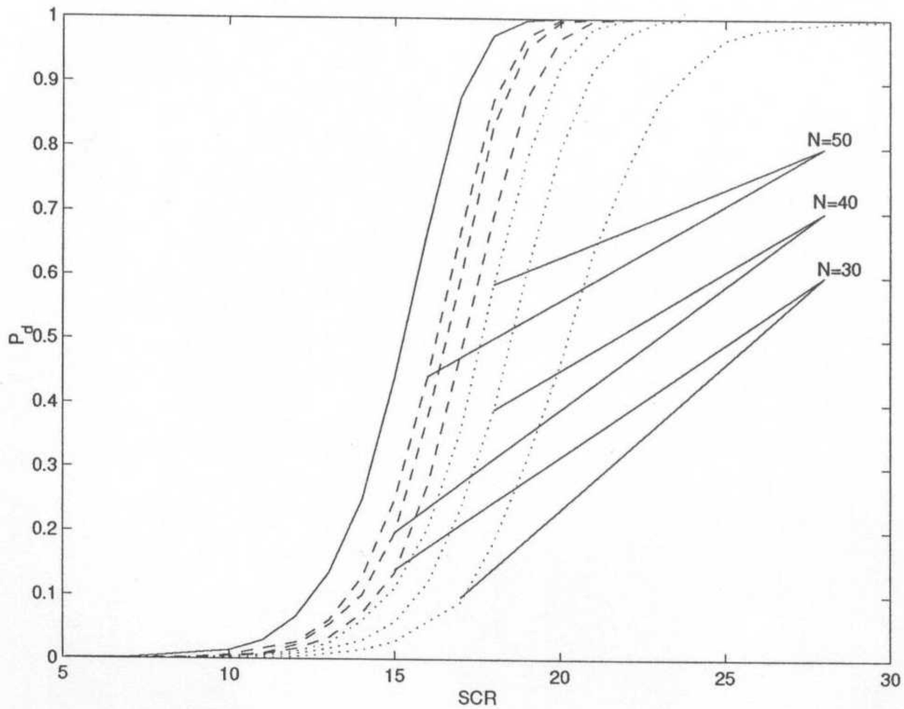

Figure 3a. P_d versus SCR of the receiver (25) (dashed curve), (27) (dotted curve), and asymptotic performance $N = \infty$ (solid curve), for $P_{fa} = 10^{-4}$, $f_d = 0.03$, $H = 10$, $M = 3$, $M_0 = 6$, target model M_1, and N as a parameter.

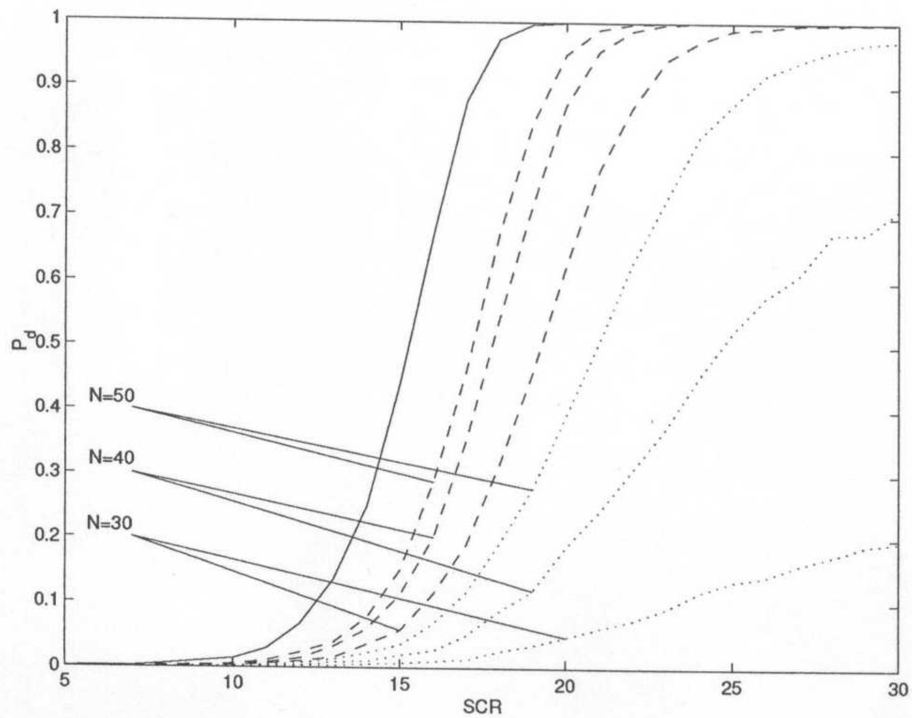

Figure 3b. P_d versus SCR of the receiver (25) (dashed curve), (27) (dotted curve), and asymptotic performance $N = \infty$ (solid curve), for $P_{fa} = 10^{-4}$, $f_d = 0.03$, $H = 10$, $M = 3$, $M_0 = 6$, target model M_2, and N as a parameter.

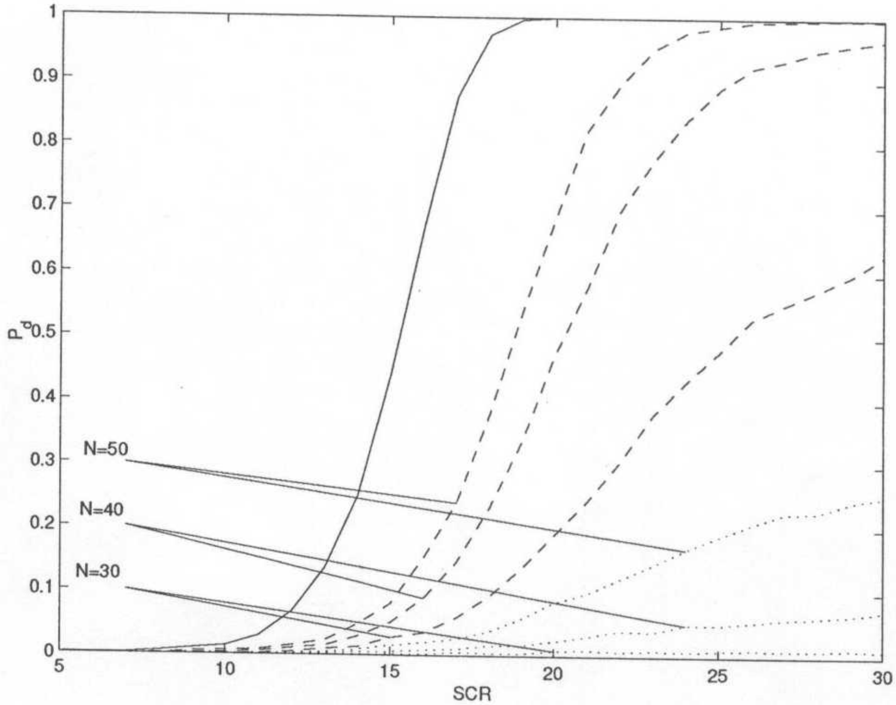

Figure 3c. P_d versus SCR of the receiver (25) (dashed curve), (27) (dotted curve), and asymptotic performance $N = \infty$ (solid curve), for $P_{fa} = 10^{-4}$, $f_d = 0.03$, $H = 10$, $M = 3$, $M_0 = 6$, target model M_3, and N as a parameter.